Journal of Human Evolution 57 (2009) 538–554

Contents lists available at ScienceDirect

Journal of Human Evolution

journal homepage: www.elsevier.com/locate/jhevol

Descriptions of the lower limb skeleton of *Homo floresiensis*

W.L. Jungers [a,*], S.G. Larson [a], W. Harcourt-Smith [b], M.J. Morwood [c,f], T. Sutikna [d], Rokhus Due Awe [d], T. Djubiantono [e]

[a] *Department of Anatomical Sciences, Stony Brook University Medical Center, School of Medicine, Stony Brook, NY 11794-8081, USA*
[b] *Department of Vertebrate Paleontology, American Museum of Natural History, New York, NY, USA*
[c] *GeoQuEST Research Centre, School of Earth and Environmental Sciences, University of Wollongong, Wollongong, NSW 2522, Australia*
[d] *Indonesian Centre for Archaeology, Jl. Raya Condet Pejaten No. 4, Jakarta 12001, Indonesia*
[e] *The National Research and Development Centre for Archaeology, Jakarta, Indonesia*
[f] *Archaeology and Palaeoanthropology, School of Human and Environmental Studies, University of New England, Armidale, New South Wales 2351, Australia*

ARTICLE INFO

Article history:
Received 18 January 2008
Accepted 1 August 2008

Keywords:
Homo floresiensis
Os coxae
Femur
Tibia
Fibula
Patella
Foot bones

ABSTRACT

Bones of the lower extremity have been recovered for up to nine different individuals of *Homo floresiensis* – LB1, LB4, LB6, LB8, LB9, LB10, LB11, LB13, and LB14. LB1 is represented by a bony pelvis (damaged but now repaired), femora, tibiae, fibulae, patellae, and numerous foot bones. LB4/2 is an immature right tibia lacking epiphyses. LB6 includes a fragmentary metatarsal and two pedal phalanges. LB8 is a nearly complete right tibia (shorter than that of LB1). LB9 is a fragment of a hominin femoral diaphysis. LB10 is a proximal hallucal phalanx. LB11 includes pelvic fragments and a fragmentary metatarsal. LB13 is a patellar fragment, and LB14 is a fragment of an acetabulum. All skeletal remains recovered from Liang Bua were extremely fragile, and some were badly damaged when they were removed temporarily from Jakarta. At present, virtually all fossil materials have been returned, stabilized, and hardened. These skeletal remains are described and illustrated photographically. The lower limb skeleton exhibits a uniquely mosaic pattern, with many primitive-like morphologies; we have been unable to find this combination of ancient and derived (more human-like) features in either healthy or pathological modern humans, regardless of body size. Bilateral asymmetries are slight in the postcranium, and muscle markings are clearly delineated on all bones. The long bones are robust, and the thickness of their cortices is well within the ranges seen in healthy modern humans. LB1 is most probably a female based on the shape of her greater sciatic notch, and the marked degree of lateral iliac flaring recalls that seen in australopithecines such as "Lucy" (AL 288-1). The metatarsus has a human-like robusticity formula, but the proximal pedal phalanges are relatively long and robust (and slightly curved). The hallux is fully adducted, but we suspect that a medial longitudinal arch was absent.

© 2008 Elsevier Ltd. All rights reserved.

Introduction

In the original description and diagnosis of *Homo floresiensis* (Brown et al., 2004), several hind-limb postcranial skeletal elements were highlighted and described. Analysis of the bony pelvis suggested that the type specimen (LB1) was a female, and the degree of lateral iliac flaring was described as "marked" in comparison to modern humans. The femur of LB1 was said to be robust and circular in cross-section and lacking a pilaster; the femoral neck was described as compressed anteroposterially, the bicondylar angle was reported as relatively high (~14 degrees), and muscle markings were characterized as "not well-developed." The lesser trochanter and intertrochanteric crest of the femur were noted as very prominent. The tibia of LB1 was characterized as robust and slightly curved along its long axis, and the midshaft was described as oval in cross-section. Overall postcranial morphology was concluded to be consistent with human-like, obligate bipedalism.

The initial report was followed by a second paper (Morwood et al., 2005) that described additional postcrania of LB1 as well as a new tibia (LB8) of another individual even smaller than LB1. This new tibia was also characterized as very robust and oval in cross-section at midshaft. With the recovery of a humerus for LB1, interlimb proportions were assessed for the first time and were found to be similar to *Australopithecus* and distinct from humans and early *Homo erectus* (also see Argue et al., 2006; Jungers, 2009). Shaft and articular dimensions of all the major limb bones were argued to be robust relative to lengths. Table 1 of Morwood et al. (2005) also listed a complete left fibula of LB1, a child's tibia (LB4/2), a femoral shaft fragment (LB9), a fragmentary metatarsal (LB6/5), and some phalanges of the foot (LB6/6, LB6/13). Morwood et al. concluded that LB1 "is not just an aberrant or pathological individual, but is

* Corresponding author.
E-mail address: williamjungers@yahoo.com (W.L. Jungers).

0047-2484/$ – see front matter © 2008 Elsevier Ltd. All rights reserved.
doi:10.1016/j.jhevol.2008.08.014

Table 1
Hind-limb elements attributed to *Homo floresiensis*

Sector	Spit	ID	Element	Age (ka)[a]	Age Rationale[b]
IV	47R	LB10	Pedal phalanx, proximal 1st	~74 $^{+14/-12}$	~LB-JR-8a
IV	52L	LB11/1	Metatarsal fragment	~74 $^{+14/-12}$	~LB-JR-8a, <LBS4-32
IV	53L	LB11/2	Pelvic fragments	~74 $^{+14/-12}$	~LB-JR-8a, <LBS4-32
IV	54L	LB11/3	Pelvic and costal fragments	~74 $^{+14/-12}$	~LB-JR-8a, <LBS4-32
XI	43	LB4/2	Tibia, right	>15.7–17.1, <17.1–18.7	>ANUA-23610, <ANUA-27117
XI	51	LB6/6	Pedal phalanx, proximal	>15.7–17.1, <17.1–18.7	>ANUA-23610, <ANUA-27117
XI	52	LB6/13	Pedal phalanx, proximal	>15.7–17.1, <17.1–18.7	>ANUA-23610, <ANUA-27117
XI	52	LB6/15	Pedal phalanx, middle	>15.7–17.1, <17.1–18.7	>ANUA-23610, <ANUA-27117
VII	54	LB13	Patella fragment	>15.7–17.1, <17.1–18.7	>ANUA-23610, <ANUA-27117
XI	57A	LB1/58	Phalanx, shaft fragment	17.1–18.7, 17.9–19.0	ANUA-27116, 27117
XI	58A	LB1/53	Fibula, left	17.1–18.7, 17.9–19.0	ANUA-27116, 27117
XI	58A	LB1/54	Talus, right	17.1–18.7, 17.9–19.0	ANUA-27116, 27117
XI	58A	LB8/1	Tibia, right	17.1–18.7, 17.9–19.0	ANUA-27116, 27117
VII	59	LB1/7	Ossa coxae	17.1–18.7, 17.9–19.0	ANUA-27116, 27117
VII	59	LB1/8	Femur, right	17.1–18.7, 17.9–19.0	ANUA-27116, 27117
VII	59	LB1/9	Femur, left	17.1–18.7, 17.9–19.0	ANUA-27116, 27117
VII	59	LB1/10	Patella, right	17.1–18.7, 17.9–19.0	ANUA-27116, 27117
VII	59	LB1/11	Patella, left	17.1–18.7, 17.9–19.0	ANUA-27116, 27117
VII	59	LB1/12	Tibia, left	17.1–18.7, 17.9–19.0	ANUA-27116, 27117
VII	59	LB1/13	Tibia, right	17.1–18.7, 17.9–19.0	ANUA-27116, 27117
VII	59	LB1/14	Fibula, right	17.1–18.7, 17.9–19.0	ANUA-27116, 27117
VII	59	LB1/15	Talus, left	17.1–18.7, 17.9–19.0	ANUA-27116, 27117
VII	59	LB1/16	Navicular, left	17.1–18.7, 17.9–19.0	ANUA-27116, 27117
VII	59	LB1/17	Cuboid, left	17.1–18.7, 17.9–19.0	ANUA-27116, 27117
VII	59	LB1/18	Entocuneiform, left	17.1–18.7, 17.9–19.0	ANUA-27116, 27117
VII	59	LB1/19	Ectocuneiform, left	17.1–18.7, 17.9–19.0	ANUA-27116, 27117
VII	59	LB1/20	Mesocuneiform, left	17.1–18.7, 17.9–19.0	ANUA-27116, 27117
VII	59	LB1/21	Metatarsal I, left	17.1–18.7, 17.9–19.0	ANUA-27116, 27117
VII	59	LB1/22	Metatarsal II, left	17.1–18.7, 17.9–19.0	ANUA-27116, 27117
VII	59	LB1/23	Metatarsal III, left	17.1–18.7, 17.9–19.0	ANUA-27116, 27117
VII	59	LB1/24	Metatarsal IV, left	17.1–18.7, 17.9–19.0	ANUA-27116, 27117
VII	59	LB1/25	Metatarsal V, left	17.1–18.7, 17.9–19.0	ANUA-27116, 27117
VII	59	LB1/26	Navicular, right	17.1–18.7, 17.9–19.0	ANUA-27116, 27117
VII	59	LB1/27	Cuboid, right	17.1–18.7, 17.9–19.0	ANUA-27116, 27117
VII	59	LB1/28	Ectocuneiform, right	17.1–18.7, 17.9–19.0	ANUA-27116, 27117
VII	59	LB1/29	Metatarsal I, right	17.1–18.7, 17.9–19.0	ANUA-27116, 27117
VII	59	LB1/30	Metatarsal II, right	17.1–18.7, 17.9–19.0	ANUA-27116, 27117
VII	59	LB1/31	Metatarsal III, right	17.1–18.7, 17.9–19.0	ANUA-27116, 27117
VII	59	LB1/32	Metatarsal IV, right	17.1–18.7, 17.9–19.0	ANUA-27116, 27117
VII	59	LB1/33	Metatarsal V, right	17.1–18.7, 17.9–19.0	ANUA-27116, 27117
VII	59	LB1/34	Pedal phalanx, proximal	17.1–18.7, 17.9–19.0	ANUA-27116, 27117
VII	59	LB1/35	Pedal phalanx, proximal	17.1–8.7, 17.9–19.0	ANUA-27116, 27117
VII	59	LB1/36	Pedal phalanx, proximal	17.1–18.7, 17.9–19.0	ANUA-27116, 27117
VII	59	LB1/37	Pedal phalanx, proximal	17.1–18.7, 17.9–19.0	ANUA-27116, 27117
VII	59	LB1/38	Pedal phalanx, proximal	17.1–18.7, 17.9–19.0	ANUA-27116, 27117
VII	59	LB1/39	Pedal phalanx, middle	17.1–18.7, 17.9–19.0	ANUA-27116, 27117
VII	59	LB1/41	Pedal phalanx, proximal	17.1–18.7, 17.9–19.0	ANUA-27116, 27117
VII	59	LB1/43	Pedal phalanx, distal	17.1–18.7, 17.9–19.0	ANUA-27116, 27117
VII	59	LB1/56	Pedal phalanx, middle	17.1–18.7, 17.9–19.0	ANUA-27116, 27117
VII	59	LB1/57	Pedal phalanx, distal	17.1–18.7, 17.9–19.0	ANUA-27116, 27117
XI	65B	LB9	Femur fragment	~18.2–19.7	~ANUA-31229
VII	69	LB14	Pelvis fragment (acetabulum)	>18.2–19.7, <41 ± 10	>ANUA-31229, <LBS7-46

[a] ka = thousand years before present.
[b] For specific details regarding the dating samples used for the age estimates see Roberts et al. (2009: Table #).

representative of a long-term population that was present during the interval 95–74 to 12 thousand years ago" (2005: 1012).

This conclusion notwithstanding, Jacob et al. (2006) attempted to dismiss these new fossils as pathological, pygmoid, Australomelanesian humans. Rather than robust, the long bones were said to be "overtubulated" and thin-walled. Weak muscle attachment sites were inferred to mean "severe muscle hypotonia (paresis)." The proximal femora and patellae were claimed to be pathologically asymmetrical, and the oval cross-sections of the tibiae were interpreted to suggest "compromise between the need to move body mass and generally weak muscle development" (Jacob et al., 2006: 13425). A few additional descriptive notes on the lower extremity were made in the Supplementary Online Materials that accompanied the main text. Claims were made there about asymmetrical sciatic notches, iliac flaring was related somehow to microcephaly, and tibial shafts were characterized as infantile. Unspecified foot bones were mentioned in passing.

Argue et al. (2006) noted that the body proportions and details of the skeletal anatomy of LB1 could not be matched in individuals diagnosed with a type of primordial dwarfism known as MOPD II. There are no signs of metaphyseal flaring or triangular epiphyses in the long bones of LB1; the bones are not thin. Disproportionate shortening of the forearm also does not characterize LB1, and the pelvis is not high and narrow, nor does it have small iliac wings and flattened acetabula. Rauch et al. (2008) simply ignored these observations in their facile speculation that LB1 suffered from MOPD II.

Another specific pathological diagnosis was offered to account for the unusual skeletal features seen in *Homo floresiensis*. Hershkovitz et al. (2007) proposed that LB1 probably suffered from a form of congenital deficiency of insulin-like growth factor known clinically as Laron Syndrome. Deviating from the classic diagnostic features for Laron Syndrome, these authors speculated that the degree of lateral flare of the iliac blade, the high bicondylar angle of the femur, the femoral neck-shaft angle, and the degree of tibial curvature seen in

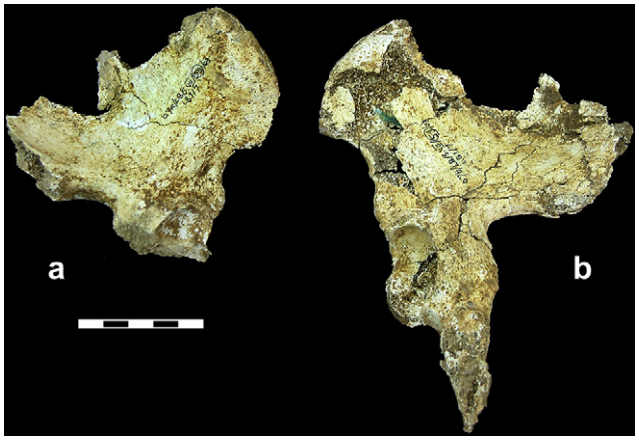

Figure 1. Posterolateral views of the fragmentary right (a) and more complete left (b) ossa coxae of *Homo floresiensis* (LB1/7).

LB1 could all be found in untreated patients afflicted with Laron Syndrome. Most of these claims lacked quantitative support, and virtually all have been challenged (Falk et al., 2008).

The goal of this paper is to describe the lower limb skeletal elements attributed to *Homo floresiensis* (Table 1). In so doing, we will revisit and expand upon the initial descriptions. We do not offer detailed functional inferences here, but we do make selected comparisons to modern humans, extant apes, and other fossil hominins in order to provide context and to highlight the unusual combination of features seen in *H. floresiensis.* When appropriate, we critique speculations about pathology (e.g., degrees of left-right asymmetry, cortical bone thickness), but a full rebuttal to these diverse claims of pathology is beyond the scope of this contribution.

LB1 lower limb elements

Ossa coxae (LB1/7)

In the original announcement of the discovery of *Homo floresiensis*, Brown et al. (2004) figure a relatively complete left os coxae (missing the pubis) of the type specimen LB1 and mention a more fragmentary right os coxae of the same individual. The left iliac crest was missing posterior to the iliac tubercle, but a portion of the inferior ischiopubic ramus remained in place. The acetabulum, ischial tuberosity, sciatic notch, and auricular surfaces were quite well-preserved. The ischial spine was originally present but was described as "not particularly pronounced," and the ilium was said to exhibit "marked lateral flare" relative to the plane of the acetabulum. The partial right os coxae is represented by the ilium alone, but does preserve the anterior inferior iliac spine, the anterior margin of the auricular surface, and some surface morphology of the blade. Only the cranial part of the acetabulum on the right side was preserved, and the iliac crest posterior to the iliac tubercle was again lacking. Regrettably, after a controversial trip to Yogyakarta (Culotta, 2005), the left bony pelvis was returned in several pieces and required extensive reconstruction to repair severe damage and pervasive cracking (Figs. 1–4). A significant portion of the bony table was lost on the gluteal surface of the left iliac blade, but it was possible to restore much of the left side to something resembling its original form. The ischial spine is now broken away completely and the inferior ischiopubic ramus is missing (along with sacral fragments mentioned in the initial report). The sciatic notch is slightly fragmented and displaced, and its smooth contour could not be restored to its original pristine state (Fig. 4). Cracks now run vertically and horizontally across the iliac blade; there is also a large crack across the acetabulum that partially separates the ilium from the ischium. Deep portions of the acetabulum are fragmented and partially displaced (Fig. 3).

Both ilia sport an iliac pillar or acetabulo-cristal buttress that is positioned relatively anteriorly, as in many hominins, but it is relatively weakly developed (not unlike the variable location and expression seen in many modern humans). A small iliac (cristal) tubercle is preserved on the crests of both ilia. The region above the auricular surface for the iliac tuberosity has been crushed and thereby obscured. The surface cracking and damage to the iliac blade prevent confident identification of the gluteal lines. The margin of the obturator foramen is sharp from just below the acetabulum to the edge of the broken ischiopubic ramus. There is a pronounced groove for the obturator internus muscle just cranial to the upper margin of the ischial tuberosity. The ischial tuberosity itself is eroded at its margins, and its width can only be approximated (Table 2). The pubis is broken away just anterior to the acetabulum. The anterior margin of the triangular auricular surface is lipped prominently, but the posterior edge is now slightly eroded (Fig. 2). The anterior inferior iliac spine is well-preserved and

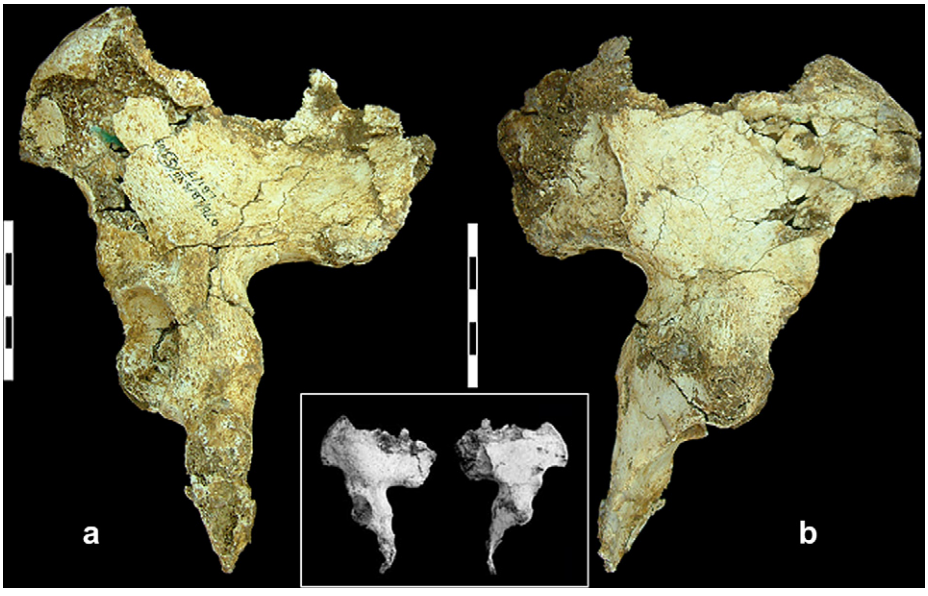

Figure 2. External (a) and internal (b) views of the restored left os coxae of LB1/7. The inset is from Brown et al. (2004) and serves to reveal areas of damage since its initial discovery.

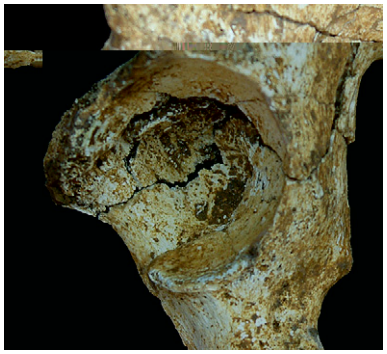

Figure 3. View of the acetabulum from the left os coxae of LB1/7. The form is typically human.

moderately developed; the anterior superior and posterior inferior iliac spines have suffered a minor degree of bone loss via surface erosion.

Without an associated pubic symphysis or sacrum, it is difficult to establish a midline for orientation of the bony pelvis confidently. However, if one articulates casts of the sacra of australopithecines such as either AL 288-1 ("Lucy") or STS 14 (or a sacrum from a *very* small human) with LB1/7 in order to establish anatomical planes, one can better assess the degree of lateral iliac flare. The anterior margin of "Lucy's" sacrum fits remarkably well with the anterior edge of LB1/7's auricular surface (Fig. 4). The iliac blade flares strongly beyond the margin of the acetabulum, thereby confirming Brown et al.'s (2004) original observations. This degree of iliac flaring is not a function of the sacrum with which it is paired; rather, it is intrinsic to the os coxae and resembles that seen in australopithecines (McHenry, 1975; Stern and Susman, 1983) but not in modern humans (Arsuaga et al., 1999; Lovejoy, 2005). Overall pelvic shape is therefore consistent with the expectations for a small-bodied hominin with a very small cranial capacity (cf. Tague and Lovejoy, 1986). We do not find the radiographic and CT-scan figures in Hershkovitz et al. (2007) that purport to show comparable iliac flaring in individuals afflicted with Laron Syndrome to be convincing.

The right os coxae does not permit many useful measurements, but metric aspects of the left os coxae are presented in Table 2. Total pelvic height (from the iliac tubercle to the anteroinferior edge of the ischial tuberosity) is at least 165 mm; this is indeed a small bony pelvis, but it can easily be matched in skeletal samples of African pygmies [e.g., the Akka female, No. 1887-12-1-106 described by Flower (1889), measures only 152 mm] and in Andaman Islander skeletons in the collections of the Natural History Museum (London). The same can be said for iliac length and iliac breadth. The breadth to length ratio of the ilium of LB1/7 is 1.17, and this shape index also falls well within the range of small-bodied

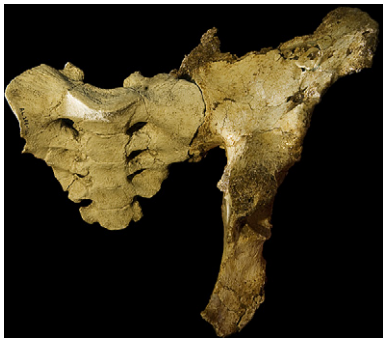

Figure 4. The left os coxae (LB1/7) is seen here articulated with a cast of the sacrum of AL 288-1 (*Australopithecus afarensis*) to permit anatomical orientation. Note the marked degree of lateral iliac flaring beyond the acetabulum, recalling the shape of australopithecine bony pelves.

Table 2
Selected measurements (mm) of the bony pelvis in *Homo floresiensis* (LB1/7, left side)

Total (maximum) pelvic height	165
Iliac height (from center of acetabulum)	105
Maximum iliac breadth	123
Thickness of iliac crest at tubercle	11
Sciatic notch to anterior inferior iliac spine	46
Ischial length (from center of acetabulum)	~55
Ischial shank length (edge of acetabulum to superior edge of tuberosity)	~15
Breadth of ischial tuberosity	>19
Acetabulum height (superoinferior)	36[a]
Acetabulum depth	~21
Length of auricular surface	42
Width of auricular surface	23

[a] Brown et al. (2004) report a value of 36 mm for acetabular "width".

humans (e.g., the Akka female presents a value of 1.16, whereas another African pygmy female, P4, in the collection of the Department of Anthropology, University of Geneva, has a ratio of 1.23; also see McHenry, 1975). The ratio of ischial length to iliac length is 0.52 in LB1/7, and this proportionality is also well within the range seen in African pygmies and other groups (e.g., the Akka female has a value of 0.51, whereas P4 exhibits a value of 0.56).

Joint size appears to be absolutely and relatively small in LB1/7. The superoinferior diameter ("height") of the left acetabulum is only 36 mm, which precisely matches Brown et al.'s (2004) value for an acetabular "width" of 36 mm. The smallest acetabulum of a modern human of which we are aware comes again from Flower's Akka female at 40 mm, but the same dimension in *Australopithecus afarensis* (AL 288-1) is only 35 mm (Johanson et al., 1982). If relative acetabulum size is taken as this diameter divided by total (maximum) pelvic height, LB1/7 has a ratio of 0.22, the Akka female is 0.26, and AL 288-1 is 0.22. The long axis ("length") of the auricular surface in LB1/7 measures 42 mm; although damaged, this dimension in AL 288-1 is also approximately the same. The anatomy of the acetabulum is decidedly human-like. The acetabular notch is broad, and there is a well-buttressed but eroded bony margin. As is characteristic of bipedal hominins, the superior portion of the lunate articular surface is broader than the breadth across the posterior horn. The fully developed anterior horn is human-like and distinguishes it from AL 288-1 in this important respect (Stern and Susman, 1983).

Based on the original, undistorted left greater sciatic notch of the LB1/7 os coxae, Brown et al. (2004) described it as "broad" and probably indicative of a female sex. It is true that a wide sciatic

Figure 5. The greater sciatic notch of LB1/7. Despite the cracks and slight displacement of the fragments, angular measurements support the conclusion that LB1 was a female.

notch is often useful in sorting male and female bony pelves, but there is a great deal of age-related and ethnic variation among humans in this feature (e.g., Singh and Potturi, 1978; Walker, 2005). Application of modern human sexing standards to fossil hominins requires additional assumptions (Hager, 1996), and misclassification of males based on the greater sciatic notch alone is common (Walker, 2005). The greater sciatic notch of LB1/7 is now slightly distorted (Fig. 5), and the ischial spine is broken. Given these caveats, if one attempts to calculate the total angle and "posterior angle" of the greater sciatic notch after Takahashi (2006), the conclusion that LB1 was a female seems very reasonable. The total angle is approximately 79 degrees in LB1/7 and the posterior angle is 38 degrees. The former value is just below the optimal cutoff point for separating males (lower values) from females (larger values), and is therefore inconclusive; however, the posterior angle is much larger than the optimal cutoff point (i.e., clearly female) and represents a high value that was never observed in the large male sample measured by Takahashi (2006). Although LB1 appears to have been the largest individual recovered to date for *Homo floresiensis*, she was probably a female. The sciatic notch of the right os coxae of LB1/7 is too fragmentary to measure and compare to the left in any meaningful way (i.e., left-right sciatic notch asymmetry cannot be assessed) (Jacob et al., 2006).

Femora (LB1/8 and LB1/9)

Both left and right femora are represented in the skeleton of LB1 (Figs. 6 and 7). LB1/9 is a left femur and the more complete of the two. A typographical error in Brown et al. (2004) inadvertently listed this femur as a right; this error was corrected in Jacob et al. (2006). It is noteworthy that these bones bear very little resemblance to modern human femora excavated from more recent archeological sites on Flores Island (Verhoeven, 1958; Jacob, 1967; van der Plas, 2007). The right femur (LB1/8) is missing the top of the greater trochanter; it appears to have been sheared off. The head is also broken off about midway along the femoral neck. A groove for the tendon of the obturator externus muscle is palpable across the posterior surface of the neck. There are several large cracks in the diaphysis, including a horizontal crack along the anterior surface at the level of the lesser trochanter. A postmortem crack at midshaft and another one roughly three-quarters down the shaft have been repaired, and the pieces have been re-glued. The posterior aspect reveals a prominent intertrochanteric crest, and a well-defined lesser trochanter that faces posteromedially. The right lesser trochanter *appears* to project more medially than on the left femur (LB1/9) because, without a femoral head, the right shaft rotates externally when placed on a flat surface (Fig. 7); this is the apparent basis for the erroneous claim that the lesser trochanters of LB1/8 and LB1/9 are highly asymmetrical in position and size (Jacob et al., 2006). The proximal portion of the patellar articular surface is preserved and measures just over 32 mm in breadth. The distal end is damaged, apparently through crushing; approximately 257 mm of the femur remains. The medial condyle is compressed in the anteroposterior plane, and its articular surface is abraded; the anteroposterior dimension of what remains is just over 34 mm. The lateral condyle is broken off just below its epicondyle, and the intercondylar notch is still full of matrix. Although there is no femoral pilaster (Brown et al., 2004), and contrary to the exaggerated characterization by Jacob et al. (2006), there is indeed a well-defined linea aspera on the posterior surface of the shaft; the gluteal tuberosity is also present as a prominent rugosity that forms the upper lateral branch of the linea aspera. The spiral line is also well-developed, emerging just inferior to the lesser trochanter and merging with the short but very visible linea aspera. The expression of the linea aspera in modern humans is highly variable (Hrdlicka, 1934). A modestly developed linea aspera without an associated pilaster need not imply anything about reduced muscularity and activity levels (contra Jacob et al., 2006). Rather, this combination is reported to be correlated with increased shaft robusticity – a well-documented feature of LB1 (Morwood et al., 2005) – and occurs as a rule in Neandertals (Trinkaus, 1983, 2006). The linea aspera is short in LB1 because the diaphysis of the femur itself is also absolutely and relatively short (see below). This creates the impression of an enlarged popliteal surface because the inferior branches of the linea aspera diverge after having fully merged for only a short distance. This is a secondary effect of a very short femur, and not evidence of pathology or disordered development. The expression of the linea aspera also varies considerably within more ancient

Figure 6. Anterior views of the right (a, LB1/8) and left (b, LB1/9) femora of the type specimen.

Figure 7. Posterior views of the right (a, LB1/8) and left (b, LB1/9) femora of the type specimen.

hominins, and one need not invoke reduced muscularity or compromised motor function to explain this variation. For example, some *Australopithecus afarensis* individuals (e.g., A.L.288-1) exhibit a "minimal linea aspera" morphology, and the older Asa Issie femur (ASI-VP-5/154) lacks a linea aspera altogether (White et al., 2006); we suspect that ambulation in these fossils was not impaired by this anatomy.

The surface morphology and geometry of the left femur (LB1/9) is very similar to that described above for the right side, but the left femur is more complete, especially proximally. At 280 mm in total interarticular length (Brown et al., 2004), LB1/9 is shorter than any modern human femur of which we are aware, including African pygmies and Andaman Islanders; it is, however, remarkably close in length to the reconstructed femur of AL 288-1 ("Lucy") (e.g., Jungers, 1982). The head and greater trochanter are relatively well-preserved on LB1/9. The head is missing a small, superior-most sector of the articular surface, and matrix slightly obscures the anterior margin; accordingly, it is not possible to comment on overall articular coverage of the femoral head. The fovea capitis for the ligamentum teres is represented by a shallow depression. The average of the superoinferior and anteroposterior femoral head diameters is 31.0 mm (Table 3), a value that is intermediate between AL 288-1ap and that of the smallest-bodied modern humans (see Fig. 8). There is a fragment of bone missing from the anteroinferior aspect of the femoral neck. The neck has suffered a post-mortem fracture; even after repair, a prominent posterior crack remains evident. There is also slight damage to, and minor erosion of, the anterosuperior section of the greater trochanter. The greater trochanter of LB1/9 presents with a prominent lateral apophysis, a morphology that characterizes the femora of the genus *Homo*

er erior

Accordingly, claims of excessive femoral asymmetry (including qualitative assessments of the lesser trochanter and intertrochanteric crest) have no basis in fact and cannot be used to bolster faulty inferences of systemic bony pathology and disordered growth (Jacob et al., 2006).

Brown et al. (2004) published a neck-shaft (collodiaphyseal) angle of 130 degrees for LB1/9. Our independent value of 128 degrees is very close to this and probably within expected ranges of interobserver error. An angle of 128–130 degrees is close to the mean for many modern human groups and within the observed ranges of virtually all others, including urban dwellers, agriculturalists, and hunter-gatherers/foragers (Grine et al., 1995). Earlier fossil hominins tend to have somewhat lower values, but the upper limits of the ranges reported for *Homo erectus* and Neandertals are very close to LB1 (Grine et al., 1995). Interestingly, the neck-shaft angle for the "proto-Negrito" described by Verhoeven (1958; also see van der Plas, 2007) from another cave site on Flores Island (Liang Toge) appears to be much higher. The reported similarity in neck-shaft angles between LB1 and humans suffering from Laron Syndrome is therefore irrelevant (Hershkovitz et al., 2007). Brown et al. (2004) report a relatively high femoral bicondylar angle of 14 degrees, consistent with a relatively short femur that must approach the midline in the single support phrase of bipedal gait (Lovejoy and Heiple, 1970; Stern and Susman, 1983; Shefelbine et al., 2002). This value falls within the range reported for australopithecines, but is either at (Tardieu and Damsin, 1997) or just beyond (Shefelbine et al., 2002; Igbigbi and Sharrif, 2005) the upper end of the range seen in modern humans. Regrettably, the extensive damage to both distal femora of LB1 precludes a more complete consideration of this part of the knee joint in *Homo floresiensis*. It appears that Van Heteren (2008) confused the femoral bicondylar angle for tibial torsion.

Patellae (LB1/10 and LB1/11)

Although the distal femora of LB1 are both badly damaged, both patellae were recovered in very good (LB1/11, left) to excellent (LB1/10, right) condition (Fig. 9). LB1/10 is intact except for a slight abrasion of the inferior articular surface and the lateral margin. LB1/11 exhibits a complete horizontal fracture just above the inferior edge of the posterior articular surface, and this is also visible in anterior view. There is also a thin layer of matrix adhering to the superomedial border on the posterior articular aspect. Both patellae display a superolateral notch, a nonmetric trait useful in siding modern human patellae (Bass, 1971). Similarly, the lateral articular facet is larger than the medial, a pattern typical of modern humans (e.g., White, 1991). Maximum patellar heights are 33.1 mm (LB1/11) and 31.3 mm (LB1/10); the maximum height of LB1/11 is inflated by the residual matrix and the aforementioned transverse crack, but by no means does it approach approximately "10% longer superoinferiorly" than the LB1/10 patella even if one fails to compensate for these factors (contra Jacob et al., 2006: 13425). If one were to subtract only 1.0 mm from the height of LB1/11 in an attempt to partially correct for the crack and matrix, the absolute percentage left-right asymmetry would be less than 3%. Left-right asymmetries in maximum mediolateral width (30.9 mm for LB1/11, 30.5 mm for LB1/10) and anteroposterior thickness (12.3 mm for LB1/11, 12.1 mm for LB1/10) are even less (<2%), observations that further invalidate the assertions of abnormal growth and postcranial pathology (Jacob et al., 2006). The patellae of LB1 are long for their width in comparison to African pygmies (WLJ, pers. obs.) and many other modern humans (e.g., Bidmos et al., 2005), but this morphology can be readily matched in the large sample of human patellae from the Indian subcontinent housed in the Inke Human Osteological Collection at Stony Brook University (Department of Anatomical Sciences).

Tibiae (LB1/12, LB1/13)

The right tibia of LB1 (LB1/13) is almost complete, but the left one (LB1/12) is missing its proximal end just above the tibial tuberosity (Figs. 10 and 11). Both have obviously suffered complete cracks across the diaphysis, but these have been realigned and reglued in the restoration process. LB1/13 is lacking its medial

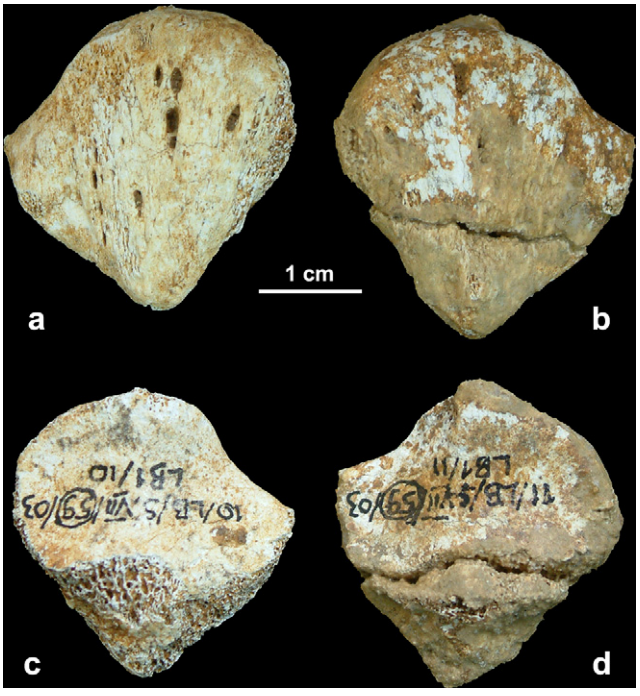

Figure 9. Right (a, c, LB1/10) and left (b, d, LB1/11) patellae of the type specimen. Anterior above, posterior below.

Figure 10. Anterior views of left (a, LB1/12) and right (b, LB1/13) tibiae of the type specimen. LB1/13 is also shown articulated (c) with its associated fibula (LB1/14).

Figure 11. Posterior views of LB1/13 (a), LB1/12 (b) and the right tibia of another individual, LB8/1 (c).

malleolus and a portion of cortical bone immediately proximal (Brown et al., 2004; Jacob et al., 2006). The maximum length of what remains of LB1/13 is 233 mm, and Brown et al. (2004) reconstruct total maximum length at approximately 235 mm; this is probably slightly too conservative if one takes into account that what remains of the medial malleolus on LB1/12 is clearly longer than 2 mm. A range of 235–240 mm seems reasonable, and this is shorter than the tibia of any modern human of which we are aware (including African pygmies and Andaman Islanders). Brown et al. (2004) report a bicondylar breadth of the tibial plateau at 51.5 mm; our measurement is slightly higher at 53.3 mm. The maximum anteroposterior diameter of the tibial plateau is 34.5 mm. Both intercondylar tubercles of the intercondylar eminence are preserved in LB1/13, and their tips are approximately 9 mm apart. The anteroposterior diameter of the medial condyle (articular surface) is 31.3 mm; the anteroposterior diameter of the lateral condyle is shorter at 25.7 mm, a discrepancy that is typical of hominins. However, the absolute articular dimensions are smaller than those of any living human that we have encountered, and more closely approximate the values seen in small individuals of *A. afarensis* (e.g., AL 288-1aq). The overall morphology of the tibial plateau appears decidedly human-like to us, but it would be valuable to check our visual assessment of condylar shape using more rigorous quantitative methods (e.g., Landis and Karnick, 2006; Organ and Ward, 2006). The articular surface of the medial condyle is moderately retroflexed – as in many hominins – with respect to the long axis of the tibial diaphysis (Martin and Saller, 1959).

LB1/13 has a prominent tibial tuberosity, and a marking that we interpret as a probable muscle scar for the insertion of the pes anserinus tendon complex inferior and medial to the tuberosity (Fig. 10). The superior fibular articular facet is flat but its margins are eroded. Brown et al. (2004) remark upon the "slight curvature in the long axis" of LB1/13, and we agree that is it is *very* slight indeed (Figs. 10 and 11), especially when viewed together with an articulated fibula. Comparably curved tibia can be found among modern humans, and we do not regard it as diagnostic of *Homo floresiensis*. The claim that this degree of tibial curvature is similar in patients with Laron Syndrome lacks quantitative support (Hershkovitz et al., 2007). Both LB1/12 and LB1/13 preserve obvious soleal lines on their posterior surfaces, although it appears more prominently on LB1/12. LB1/13 displays a prominent vertical crest proximally in the posterior midline that persists until midshaft. As accurately described by Brown et al. (2004), the shafts of both tibiae are oval in cross-section at midshaft and lack a sharp anterior border or crest. Much has been made of this observation by Jacob et al. (2006:13425); they suggest it is "an unusual feature suggesting compromise between the need to support and move body mass and generally weak muscle development." We submit that this functional inference lacks biomechanical substance. As Hrdlicka noted long ago after examining almost 2000 normal tibiae from "various nations and both sexes … The most striking peculiarity of the normal tibia is its variability in shape. The bone is hardly ever exactly alike in any two skeletons, and it will occasionally differ markedly in the same body" (1898:307). Among the types or varieties of tibial shapes (at midshaft) recognized by Hrdlicka were "those cases in which *the whole shaft is irregularly oval*" (1898:308, emphasis in the original). This describes the tibiae of LB1 perfectly. Hrdlicka frequently observed this variety among African-Americans, and we have observed it on Khoe-san tibiae in CT-scans (courtesy of F.E. Grine. Oval tibial shafts characterize African apes and *A. afarensis* (e.g., AL 288-1aq and AL 129-1b), and one can also observe non-triangular tibiae among early "anatomically modern" humans and Neandertals (Trinkaus, 1983; Trinkaus and Ruff, 1999). Inferences of pathology and unspecified "compromises" are not warranted by the observation of oval cross-sections in hominin tibiae. The anteroposterior diameter of LB1/13 at midshaft is 24.9 mm, and the mediolateral diameter is 16.9 mm. If one forms an index by dividing the latter diameter by the former, one obtains a value of 67.8%, a value slightly below the averages provided by Hrdlicka (assuming that comparable landmarks were employed). The tibiae are "robust"; i.e., their transverse diameters are large for the lengths of the bones (cf. Brown et al., 2004; Morwood et al., 2005).

Jacob et al. (2006) also claim that the cortical bone in the tibiae of LB1 are pathologically thin and indicative of long bone "overtubulation" and "disordered growth". The basis of this conclusion supposedly derives from measurements taken from CT-scans at an unspecified location on the bone; they report a value of approximately 2 mm for cortical bone thickness. They do not specify how or where this measurement was taken, although explicit protocols have been developed for extracting such data from CT-scans (and which are especially important when the medullary cavity is filled with matrix, as they are here) (Spoor et al., 1993; Coleman and Colbert, 2007). During the conservation process of LB1 and the other fragile bones of *H. floresiensis* in the summer of 2006 by Lorraine Cornish (the Natural History Museum, London), the tibiae of LB1 were unglued at their cracks near midshaft, and direct measurements of cortical bone thickness were taken with digital calipers. Anterior cortical bone thickness at these natural breaks ranged from 8.36 mm to 8.40 mm, posterior cortical bone thickness ranged from 8.47 mm to 8.56 mm, medial cortical bone thickness ranged from 5.08 mm to 5.59 mm, and lateral cortical thickness (the thinnest wall in both tibiae) ranged from 3.32 mm to 3.76 mm. Cortical indices in LB1 are all in the normal human range, and the metric claims and attendant conclusions of Jacob et al. (2006) can be firmly rejected.

As was noted above, the distal ends of both tibiae have suffered minor breakage and erosion of the outer surfaces, although this

damage is somewhat more extensive in LB1/13. The anteroposterior diameter of the distal epiphysis measures at least 21.8 mm in LB1/12, and the mediolateral diameter is greater than 26 mm. The anteroposterior diameter of the inferior fibular articular facet is approximately 17.6 mm, and the same facet in LB1/13 is 18.1 mm. The anterior surfaces of the tibial diaphyses flatten somewhat in their distal one-quarter. The posterior malleolar groove is not preserved on either tibiae of LB1. Angular torsion of the distal articular surface relative to the proximal end in LB1/13 appears positive but very low compared to most modern humans (cf. Wallace et al., 2008).

One surface feature seen on the left tibia that is not exhibited on the right tibia is an area of slightly elevated and roughened bone approximately three-quarters of the length down the shaft on the medial and anterior surfaces. We agree with the diagnosis that it might be the healed result of local trauma or a bony response to a local infection (Jacob et al., 2006).

Fibulae (LB1/14, right; LB1/53, left)

A right fibula, LB1/14, is shown with LB1/13, its associated tibia, in Fig. 10. The two fibulae are shown together in Fig. 12 and appear to be quite human-like in overall morphology. LB1/14 is 225.1 mm long, and LB1/53 is 225.3 mm long. Left-right asymmetry in length is therefore trivial. Both fibulae have been broken in several places but are now repaired and exhibit relatively little residual distortion. The proximal epiphysis of LB1/14 was originally broken off its shaft, and the proximal articular facet is present but eroded (>13 mm in M-L breadth). There is another break roughly 25% down the diaphysis from the head, and another near the distal 75% level. LB1/53 was snapped in half roughly half-way down the diaphysis, and its head was also broken off. In addition, the distal end was also fractured away from the shaft. The proximal articular facet in LB1/53 is also eroded (A-P length is approximately 13 mm). The proximal styloid processes of both fibulae are abraded at their tips. The maximum dimension of the head (M-L) is 19.5 mm in the left fibula and approximately 18.4 mm in the right fibula, with differential abrasion accounting for most of the difference in the size of the two heads.

Figure 12. Posterior view of the right fibula (a, LB1/14) and posteromedial view of the left fibula (b, LB1/53) of the type specimen.

After being repaired, both fibulae are relatively straight. A longitudinal line is visible on the anterior surfaces of both fibulae, forming a sharper ridge in the middle segment of the bones; this is the interosseous crest for attachment of the interosseous membrane. Midshaft diameters of the two fibulae are similar but not identical; the A-P diameter of LB1/14 is 10.7 mm compared to 11.0 mm in LB1/53, and the M-L diameter of LB1/14 is 8.7 mm compared to 9.3 mm in LB1/53. Midshaft circumferences are also very similar at 31.3 mm (LB1/14) and 32.5 mm (LB1/53). The middle portions of the shafts of the fibulae are relatively flat medially. The distal ends of the bones are similar in size, with an A-P diameter of 16.8 mm on the right and 16.6 mm on the left. The lateral malleoli project distally, and their posterior surfaces have well-defined peroneal grooves. The distal subcutaneous surface faces laterally (Fig. 10) as in modern humans [but unlike the anterior orientation seen in most distal fibulae of *A. afarensis* (Stern and Susman, 1983)]. The A-P diameter of the malleolar articular surface is 14.1 mm in LB1/14 and 14.5 mm in LB1/53.

Tarsus (LB1)

All tarsal elements are represented in the foot remains of LB1 except for the calcaneus (Table 4; Figs. 13–17). LB1/15 is a virtually complete left talus that is comparable in size to "Lucy" (AL 288-1as; Fig. 13) but smaller than the tali of even the smallest African pygmies (WLJ, pers. obs.). Although similar in length and width, the height of the talar body of LB1/15 is greater than in AL 288-1as. In this, and in many other respects, LB1/15 is similar to modern humans in overall morphology, but there are noteworthy exceptions, which are discussed below. The dorsal trochlear groove is shallow and the medial and lateral margins of the trochlea are similar in elevation; this shape is human-like (Harcourt-Smith and Aiello, 2004). The trochlea itself appears to be only slightly wedged (anterior width is 22.2 mm, middle width is 19.5 mm, posterior width is indeterminate due to erosion of the posterolateral margin). There is a slight indentation posteriorly that represents the flexor groove. The neck angle is 23 degrees, similar to AL 288-1as and well within the range of most modern humans (e.g., Rhoads and Trinkaus, 1977; Wallace et al., 2008). The anterior margin of the talar head is only slightly curved, much less so than is seen in AL 288-1as, and therefore is more human-like; it measures 22.6 mm in width and 16.2 mm in height. Perhaps the most remarkable aspect of LB1/15 is the very low degree of talar head torsion; at only 26 degrees, the torsion is considerably less than in AL 288-1as (36 degrees) and much less than (2 to 4 standard deviations below) the average modern human (>40 degrees; Rhoads and Trinkaus, 1977). In this respect, LB1/15 is more ape-like (Day and Wood, 1968; Gebo and Schwartz, 2006). The area on the inferior surface of the talar head corresponding to the contact for calcaneo-navicular (spring) ligament appears relatively small, but there is some postmortem bone

Table 4
Pedal remains of LB1 (*Homo floresiensis*)

Element	Measurements
Talus (left) – LB1/15	Length = 38.8 (M1 = 34.6)
Navicular (left) – LB1/16	Width = 29.7
Navicular (right) – LB1/26	Width = 29.2
Cuboid (left) – LB1/17	Length = 18.5 (medial edge)
Cuboid (right) – LB1/27	Length = 18.4 (medial edge)
Ectocuneiform (left) – LB1/19	Length = 16.9 (dorsal surface)
Ectocuneiform (right) – LB1/28	Length = 16.8 (dorsal surface)
Mesocuneiform (left) – LB1/20	Length = 11.6 (dorsal surface)
Entocuneiform (left) – LB1/18	Length = 15.4 (dorsal midline)
Metatarsal I (left) – LB1/21	Midline length = 47.0, mid-circumference = 34.60
Metatarsal I (right) – LB1/29	(Incomplete)
Metatarsal II (left) – LB1/22	Midline length = 63.0, mid-circumference = 24.80
Metatarsal II (right) – LB1/30	(Incomplete)
Metatarsal III (left) – LB1/23	Midline length = 60.4, mid-circumference = 24.53
Metatarsal III (right) – LB1/31	(Incomplete)
Metatarsal IV (left) – LB1/24	Midline length = 58.3, mid-circumference = 23.86
Metatarsal IV (right) – LB1/32	Length >53 (slightly damaged)
Metatarsal V (left) – LB1/25	(Incomplete)
Metatarsal V (right) – LB1/33	Midline length = 55.2 (without tuberosity), mid-circumference = 24.8
Proximal phalanges	
LB1/34	Max length = 21.7, mid M-L diameter = 6.59
LB1/35	Max length = 23.9, mid M-L diameter = 6.41
LB1/36	Max length = 26.2, mid M-L diameter = 6.81
LB1/37	Max length = 24.5, mid M-L diameter = 6.90
LB1/38	Max length = 26.8, mid M-L diameter = 6.53
LB1/41	(Incomplete)
Intermediate phalanges	
LB1/39	Max length = 14.7, mid M-L diameter = 5.86
LB1/56	Max length = 8.7, mid M-L Diameter = 7.18
Distal phalanges	
LB1/43	Max length = 8.5, basal width = 8.49
LB1/57	Length = 9.8, basal width = 9.80

loss in this region that complicates this assessment. The anterior and middle calcaneal articular facets are confluent. The posterior calcaneal articular facet is strongly curved along its long axis. The medial malleolar facet is oriented vertically whereas the lateral malleolar facet flares laterally, as is typical for hominins. LB1/54 is a very fragmentary right talus, preserving a portion of the trochlear surface and most of the lateral fibular facet.

The navicular of *H. floresiensis* retains a very primitive-like morphology (Fig. 14). Both left (LB1/16) and right (LB1/26) naviculars exhibit tuberosities that project appreciably medially beyond the facet for the entocuneiform, and they are quite short anteroposteriorly on their lateral sides. Anteroposterior lengths on the medial side are 13.8 mm in LB1/16 and 13.3 mm in LB1/26; its lateral lengths are 6.8 mm and 6.7 mm, respectively. This type of lateral "pinching" or wedging is seen in African apes, *A. afarensis*, and *A. africanus*, but is typically lacking in modern humans and is

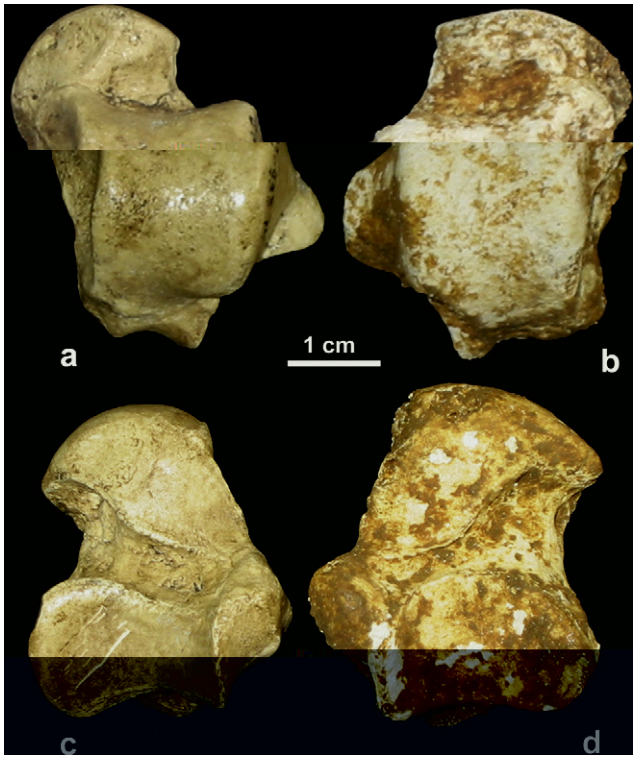

Figure 13. Superior views of the right talus of *A. afarensis* (a, AL 288-1) and left talus of the type specimen of *H. floresiensis* (b, LB1/15) above; inferior views (c, d) of same below.

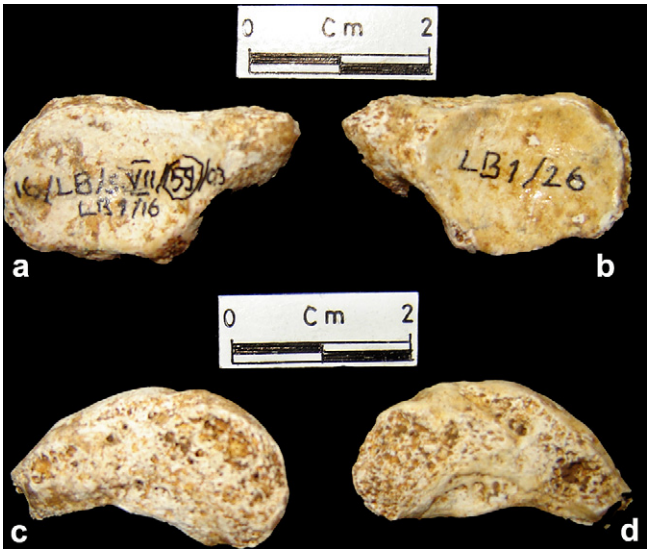

Figure 14. Proximal views of the left (a, LB1/16) and right (b, LB1/26) naviculars above; Dorsal views (c,d) of same below.

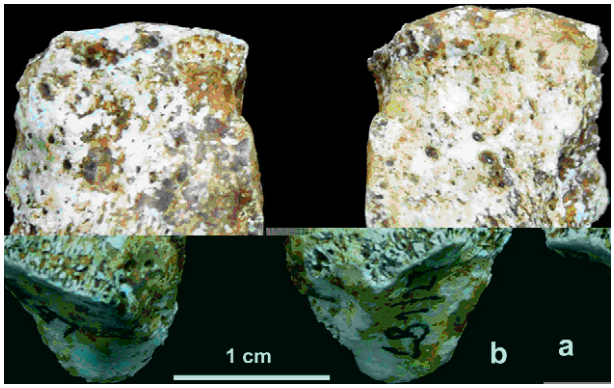

Figure 15. Dorsal views of left (a, LB1/17) and right (b, LB1/27) cuboids of the type specimen. Note the asymmetrically placed inferior calcanean process or "beak".

greatly reduced in *Homo habilis* [as represented by the OH 8 navicular (Sarmiento and Marcus, 2000; Harcourt-Smith and Aiello, 2004)]. There is a well-developed tubercle on the inferior margin that most probably represents the attachment site for the spring ligament (Susman, 1983; Sarmiento and Marcus, 2000). The maximum widths of the two naviculars are similar at 29.7 mm (LB1/16) and 29.2 mm (LB1/26); the widths of the proximal articular surface for the head of the talus are also similar at 22.6 mm and 21.3 mm, respectively. In other words, there is very little left-right asymmetry. Articular facets on the distal surface of the naviculars for the cuneiforms are visible lateral to the expanded medial tuberosity, but the cuboid appears to have been excluded from contacting this surface (also see Fig. 16). It seems likely that the navicular tuberosity was weight-bearing; a medial longitudinal arch was probably poorly developed or lacking.

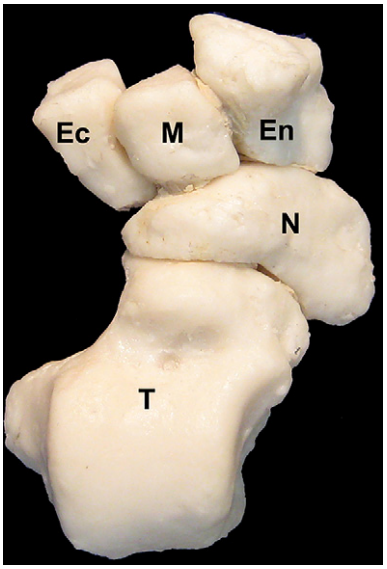

Figure 17. Articulated high resolution casts of the left talus(T), navicular (N), entocuneiform (En), mesocuneiform (M), and ectocuneiform (Ec) of the type specimen (LB1).

Both left (LB1/17) and right (LB1/27) cuboids were recovered (Fig. 15), but the lateral edges of both are slightly damaged; this contributes to the rather narrow shape of these bones (human cuboids are typically more trapezoidal in shape). The two cuboids of LB1 are very similar in length (Table 4). The distal articular facet is very flat, with little difference in angulation between the articular facets for metatarsals IV and V. The groove on the inferior surface for the tendon of the peroneus longus muscle is present in both but

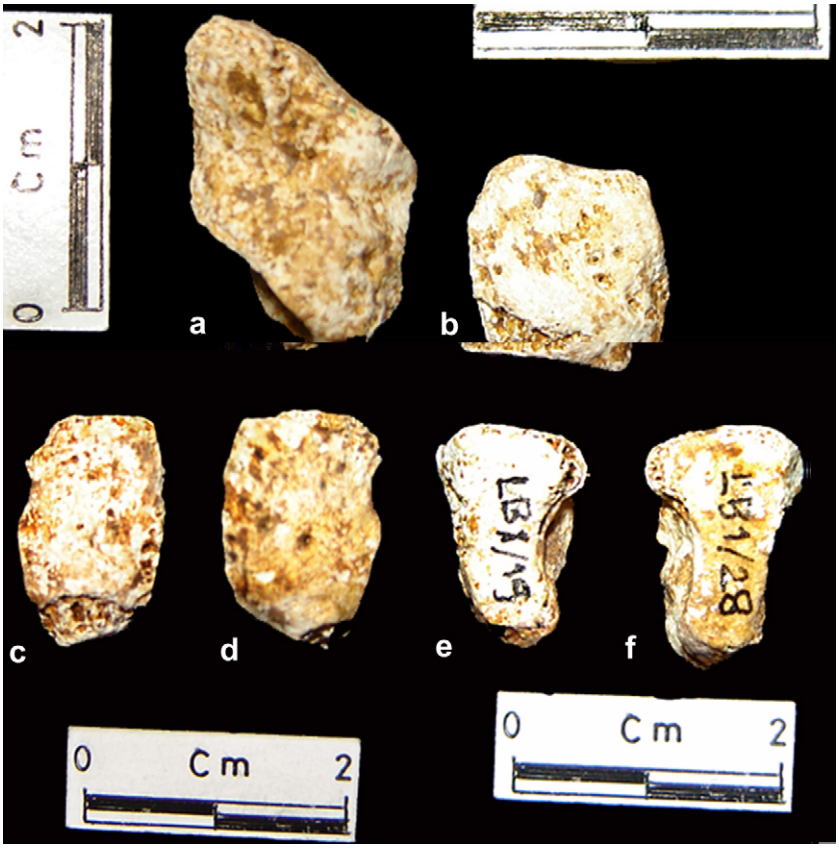

Figure 16. Dorsal views of the left entocuneiform (a, LB1/18), the left mesocuneiform (b, LB1/20), the left (c, LB1/19) and right (d, LB1/28) ectocuneiforms of the type specimen. Distal views (e, f) of the same ectocuneiforms.

appears shallow due to slight damage to the margins. There is an asymmetrically (proximomedially) placed calcanean process or "beak" on both cuboids. Although the expression of this process is variable in modern humans, it is usually regarded as the hallmark of a derived, bipedal calcaneocuboid joint that locks or close-packs in pronation late in stance phase, thereby providing a stable longitudinal lateral column (Bojsen-Moller, 1979; Susman, 1983; Kidd, 1998). Apes are also variable in the degree to which they express this "beak," but when it does occur it tends to be located closer to the median plane and affords less stability (i.e., there is no close-packed position and it serves more as a pivot) (Susman, 1983).

Additional tarsal bones include one entocuneiform (LB1/18), one mesocuneiform (LB1/20) and both ectocuneiforms (LB1/19, left; LB1/28, right) (Figs. 16 and 17). The two ectocuneiforms are almost identical in length (Table 4). Part of the entocuneiform is sheared off distolaterally, and there is a prominent osteophytic growth along the medial margin of the hallucal facet. The hallucal facet itself is very flat and forward facing; it signals a hallux that was fully adducted. The mesocuneiform facet on the lateral aspect is L-shaped and human-like. The mesocuneiform and both ectocuneiforms are also very human-like; they are rather long proximodistally relative to their respective widths. When assembled digitally, the tarsal bones reveal a well-developed transverse tarsal arch. The calcaneocuboid joint points to a stable lateral column during stance phase of walking. The degree of medial arch development is more difficult to assess without a calcaneus and in view of conflicting morphological signals. The talonavicular complex is decidedly symplesiomorphic in overall shape, but there is evidence of a reasonably well-developed spring ligament. This combination could imply a midtarsal complex that was relatively rigid longitudinally but still partially weight-bearing on the medial side of the foot.

Metatarsals (LB1)

Metatarsals were recovered from both feet of LB1, but the ones on the left side are more complete (except for the metatarsal V) (Fig. 18). The sequence of lengths from medial to lateral (Table 4) is human-like (Martin and Saller, 1959); metatarsal I is the shortest, and metatarsal II is the longest. Measuring just 47 mm in length, metatarsal I (LB1/21) is slightly longer than the hallucal metatarsal of Flower's Akka female pygmy human (43.6 mm) and *Paranthropus robustus* (SKX 5017, 43.5 mm; Susman and Brain, 1988), and it is absolutely shorter than that of most common chimpanzees (Susman and Brain, 1988). However, metatarsal I is *relatively* very short. The ratio of lengths for I/II is only 75% in comparison to average values of 82–84% in modern humans (Martin and Saller, 1959), including African pygmies and Asian "negritos" (WLJ, pers. obs.); the ratio of 75% for I/II lengths is below the observed range for humans but very similar to indices reported for female gorillas (McFadden and Bracht, 2005). Relative to metatarsal III, the relative length of the hallucal metatarsal also falls below the human range but well within the ranges of chimpanzees and gorillas (Wunderlich, 1999; McFadden and Bracht, 2005). Relative to metatarsal IV, LB1/21 again falls below the range for modern humans but comfortably within Africa ape ranges of variation (Langdon, 1986; McFadden and Bracht, 2005; WLJ, pers. obs.). While it is not uncommon for the second toe to be slightly longer than the first in

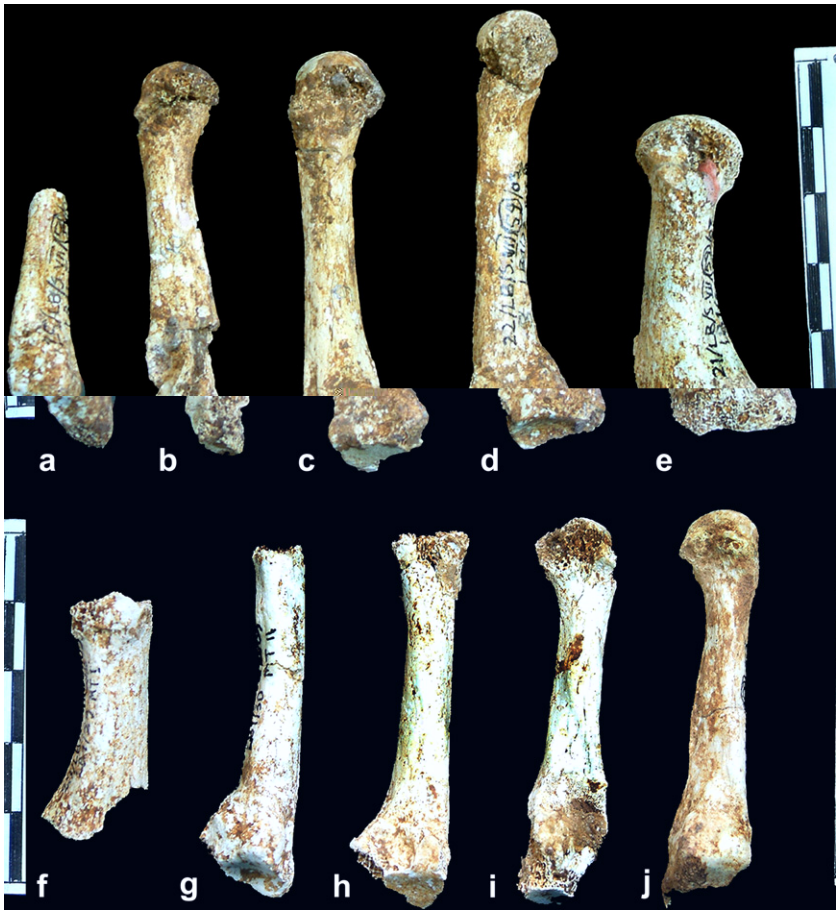

Figure 18. Top row, medial views of the left metatarsals of the type specimen (a, V – LB1/25; b, IV – LB1/24; c, III – LB1/23; d, II – LB1/22; e, I – LB1/21). Bottom row, medial views of the right metatarsals (f, I – LB1/29; g, II – LB1/30; h, III – LB1/31; i, IV – LB1/32; j, V – LB1/33).

an articulated foot (e.g., Papadopoulos and Damon, 2005), it is unlikely that the proximal and distal phalanges of the hallux in LB1 could have compensated sufficiently for the short first metatarsal to make rays I and II subequal in overall length. The functional significance of this proportional difference is unclear to us, but it is associated with a derived articular morphology of the hallucal metatarsal. Metatarsal I is a robust bone as in humans, and articular and shaft dimensions are large relative to length. The base and proximal articular surfaces are damaged medially, but the portion of the joint that remains is decidedly flat, not unlike the surface of the entocuneiform with which it articulates. It is clearly an adducted, nongrasping hallux (McHenry and Jones, 2006). The distal articular surface has a mediolateral crack running across its dorsal one-third, and the distomedial surface is missing. The distal articular surface extends onto the dorsum of the head to a considerable degree (although there is slight erosion at its dorsal limit), and it appears to be quite broad and relatively flat mediolaterally in distal and dorsal views (cf. Fig. 22); in this respect, it is more derived in the direction of modern humans than is *Paranthropus*, *A. afarensis*, and apparently early *Homo* from Dmanisi (Susman et al., 1984; Susman and Brain, 1988; Lordkipanidze et al., 2007). Enhanced mediolateral stability at hallucal toe-off seems likely. The plantar breadth of the head cannot be assessed due to damage to both margins, but it is unusual in that it lacks the paired grooves for sesamoid bones and the associated "beak" between them. Despite the dorsal broadening and flattening of the distal hallucal articular surface, the relative shortness of metatarsal I suggests that the toe-off mechanism was probably not identical to that seen in modern humans. Perhaps body weight did not shift fully from lateral to medial onto the hallux at the end of stance phase and was instead distributed over adjacent digits.

Due to damage and distortion of the lateral metatarsal heads relative to their shafts, it is difficult to assess the degree of head torsion. However, they exhibit dorsal expansion of the distal articular surfaces, suggesting a closed pack position in dorsiflexion (as in humans). Similarly, although metatarsal V clearly sports a peroneal tuberosity or styloid process, the bases of both LB1/25 and LB1/33 are damaged, and it is not possible to gauge their overall proximal robusticity. The lateral metatarsals are long relative to the tarsal bones. If one calculates metatarsal robusticity as midshaft circumference (Table 4) divided by length and π, the sequence seen in LB1 is typically human: I > V > IV > III > II (Archibald et al., 1972).

Figure 19. Top row, plantar views of proximal pedal phalanges of the type specimen a, LB1/34; b, LB1/35; c, LB1/36; d, LB1/37; e, LB1/38. Middle row (g–k), dorsal views in the same sequence. Bottom row, side views in different order (l, LB1/36; m, LB1/38; n, LB1/37; o, LB1/35; p, LB1/34).

Pedal phalanges (LB1)

The most complete proximal pedal phalanges attributed to LB1 are seen in Fig. 19 (LB1/34, LB1/35, LB1/36, LB1/37, and LB1/38). LB1/41 is a well-preserved base of another pedal phalanx (not figured). We are not confident about their side or precise positions in the lateral digits, but LB1/38 is the longest and perhaps belongs to the second ray. Their morphology departs in many ways from what is characteristic of modern humans, but it recalls the proximal pedal phalanges of *A. afarensis* in a few (but certainly not all) respects (Latimer et al., 1982). Despite their unusual and surprising appearance, we note that they are very different in overall shape, in details of morphology, and in absolute lengths from the obviously proximal manual phalanges assigned to both LB1 and LB6 (Larson et al., 2009). Two of LB1's proximal pedal phalanges exhibit what we interpret to be a form of distal articular pathology (LB1/34 and LB1/35). More specifically, the distal articular surfaces of these two bones are flattened and shifted far plantarly. LB1/34 (as well as LB1/37) also bears distal osteophytes, a condition not uncommon in the toe joints of humans and which can be activity-related (Schmitt et al., 2007). The hourglass shape so diagnostic of modern human proximal pedal phalanges (e.g., White, 1991) is not observed in any of these bones or in LB6 (see below), but it is also not observed in australopithecines (Latimer et al., 1982). All of the shafts narrow distally from the base and most expand again at the heads, but the shafts tend to be more parallel-sided than seen in modern humans. Ridges for the fibrous flexor sheaths are weakly expressed, and the plantar surfaces are convex rather than concave or flat. All of these phalanges are robust, and in lateral view one can see that the heads are quite small relative to their bases. Importantly, they are also

Figure 20. Dorsal views of intermediate and distal phalanges of LB1. They are articulated here for illustrative purposes only. Distal phalanges (a, LB1/57; b, LB1/43), middle phalanges (c, LB1/39; d, LB1/56).

Figure 21. Anterior views of immature right tibia of LB4/2 (a) and right adult tibia of LB8/1 (b).

similar to the pedal phalanx associated with LB6 (LB6/13; see below) and very different from the LB6/8 proximal manual phalanx. The articular surface is extended onto the dorsal aspect of the heads of LB1/36 and LB1/37, thereby permitting metatarsophalangeal extension late in stance phase of walking. These proximal pedal phalanges exhibit varying degrees of curvature, with included angles ranging from 16.8 degrees (LB1/37) to 18.5 degrees (LB1/36) to a high of 26.8 degrees (LB1/38). The curvatures observed in LB1/36 and LB1/37 fall within the upper range documented for modern human proximal pedal phalanges; the value seen in LB1/38 falls outside the human range and recalls the condition reported for some australopithecines (Susman et al., 1984).

There are two intermediate pedal phalanges and two distal pedal phalanges associated with LB1 (Fig. 20). Intermediate phalanges, even within the same foot, vary dramatically in modern humans, and that is also the case in LB1. LB1/39 is longer and less irregularly shaped than LB1/56, which is short and blocky. The two distal pedal phalanges (LB1/57 and LB1/43) are very short (Table 4) and lack the expansion of the apical tuft that typifies a manual distal phalanx. The middle and distal pedal phalanges are much more similar to corresponding modern human bones than are the proximal pedal phalanges of LB1.

Other lower limb elements

Tibia (LB4/2)

A right immature tibia, LB4/2, lacks both proximal and distal epiphyses (Fig. 21), and is associated with a comparably immature radius (Morwood et al., 2005; Larson et al., 2009). The diaphysis is broken in several places, and a large piece of proximolateral

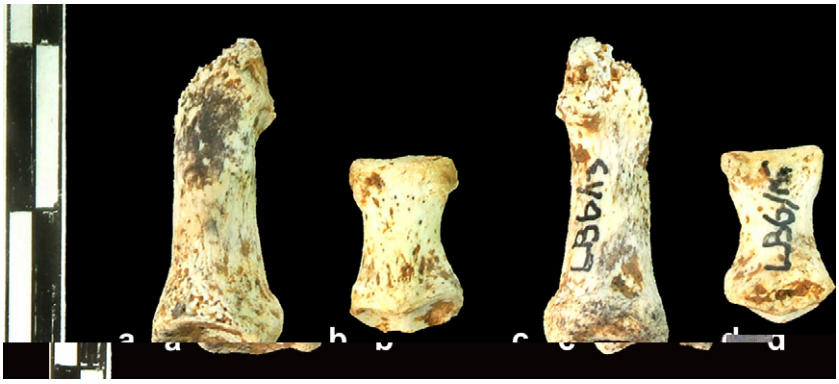

Figure 22. Dorsal views of proximal (a, LB6/13) and middle (b, LB6/15) pedal phalanges. Plantar views of same (c, d).

diaphysis is missing. The specimen measures 117 mm in length (Morwood et al., 2005). Distal to the broader proximal end, the shaft is more or less tubular and exhibits few muscle markings.

Tibia (LB8/1)

A small adult right tibia, LB8/1, is missing the medial malleolus (Figs. 11 and 21). The length of the preserved bone is 208 mm. Estimated maximum length is 216 mm (Morwood et al., 2005); this bone is from an individual even shorter than LB1 and far outside the known range for all modern humans. The lateral condyle of the tibial plateau is broken off (including the proximal articular facet for the fibula), and only a portion of the medial condyle remains intact. Part of the medial intercondylar eminence is also preserved. The tibial tuberosity is prominent, and the soleal line is clearly visible posteriorly as a nearly vertical ridge in the midline. The midshaft cross-section is oval (per Morwood et al., 2005) and lacks an interosseous crest, and the distal 20% of the diaphysis is quite flat. The oval cross-sections of both LB8/1 and LB1 tibiae indicate that this is the typical shape at midshaft for *H. floresiensis*, and should not be misconstrued as pathological or outside the known range of shapes seen in modern humans (Hrdlicka, 1898; see above). The bone is robust; at midshaft the anteroposterior diameter is 18.3 mm and the mediolateral diameter is 14.5 mm. The AP/ML index at midshaft is 79%, slightly above the mean values reported by Hrdlicka (1898). The damage done to this specimen when it was removed from the Indonesian Centre for Archeology has now been repaired. It was possible to examine cortical bone thickness near the midshaft when the separate pieces were cleaned prior to being re-glued; the cortical bone of LB8/1 is relatively thick (i.e., the cortical index is in the high normal range). The distal end of the bone measures 18.3 mm anteroposteriorly and 19.7 mm mediolaterally. A malleolar groove is present (Fig. 11), and the inferior facet for the fibula is narrow and semilunar in shape.

Figure 23. Dorsal view of proximal hallucal phalanx (LB10) articulated with head of LB1/21.

Proximal (LB6/13) and intermediate (LB6/15) pedal phalanges

Two relatively complete pedal phalanges were recovered in association with other skeletal elements of LB6 (Fig. 22). One of these is a proximal phalanx (LB6/13) and the other is an intermediate phalanx (LB6/15). There is also a very fragmentary metatarsal (LB6/5) lacking both ends (not figured). The head of LB6/13 is damaged on one side; its maximum length is just over 20 mm. The base measures 7.6 mm anteroposteriorly and 8.3 mm mediolaterally. As was seen in the proximal pedal phalanges belonging to LB1, this bone lacks the hourglass shape of modern human pedal phalanges. LB6/15 is a middle pedal phalanx that recalls LB1/39, but is shorter (11.1 mm). The base and head are similar in breadth at 7.2 mm and 7.0 mm, respectively; its midshaft breadth is 5.1 mm.

Proximal hallucal phalanx (LB10)

An isolated proximal hallucal phalanx (LB10) was recovered from Sector IV, Spit 47. It is figured in articulation with the head of the hallucal metatarsal of LB1 (LB1/22) but is treated here as a separate individual (Fig. 23). This bone is similar in form to that of modern humans but is much shorter at 24.4 mm in length. The base measures 10.0 mm anteroposteriorly and 12.6 mm mediolaterally; the head is 7.2 mm anteroposteriorly and 9.7 mm mediolaterally. Midshaft dimensions are 6.8 mm anteroposteriorly and 8.0 mm mediolaterally.

Other fragmentary postcrania

A fragment of a hominin femoral diaphysis is represented by LB9 (Morwood et al., 2005). LB11 includes badly fragmented pelvic and metatarsal bones, LB13 is a hominin patellar fragment, and LB14 is a fragmentary acetabulum. These fragments add little to the anatomical description of the hind-limb remains of *H. floresiensis*; therefore, they are not figured here nor discussed further.

Acknowledgments

Some of the costs associated with analysis of the Liang Bua hominin remains in Jakarta were covered by an Australian Research Council grant to MJM. The Wenner-Gren Foundation provided funds for the restoration and preservation of the fossils, which were performed expertly by Lorraine Cornish of the Natural History Museum (London). Support from the Leakey Foundation and the National Geographic Society is also greatly appreciated. Many thanks also go to Luci Betti-Nash for her assistance with the figures. We appreciate the constructive comments offered by Juan-Luis Arsuaga and Alejandro Bonmati on the pelvic remains of LB1. Discussions with Randy Susman about the pedal remains were extremely valuable and helpful. We also greatly appreciate the insightful comments made by three reviewers and the Editor. Editorial assistance in improving the text is greatly appreciated.

References

Archibald, J.D., Lovejoy, C.O., Heiple, K.G., 1972. Implications of relative robusticity in the Olduvai metatarsus. Am. J. Phys. Anthropol. 37, 93–96.

Argue, D., Donlon, D., Groves, C., Wright, R., 2006. *Homo floresiensis*: microcephalic, pygmoid, *Australopithecus*, or *Homo?* J. Hum. Evol. 51, 360–374.

Arsuaga, J.L., Lorenzo, C., Carretero, J.M., Gracía, A., Martínez, I., García, N., Bermudez de Castro, J.M., Carbonell, E., 1999. A complete human pelvis from the Middle Pleistocene of Spain. Nature 399, 255–258.

Auerbach, B.M., Ruff, C.B., 2006. Limb bone bilateral asymmetry: variability and commonality among modern humans. J. Hum. Evol. 50, 203–218.

Bass, W.M., 1971. Human Osteology. A Laboratory and Field Manual of the Human Skeleton. Special Publications of the Missouri Archaeological Society, Columbia, MO.

Bidmos, M.A., Steinberg, N., Kuykendall, K.L., 2005. Patella measurements of South African whites as sex assessors. HOMO 56, 69–74.

Bojsen-Moller, F., 1979. Calcaneocuboid joint and stability of the longitudinal arch of the foot at high and low gear push off. J. Anat. (Lond.) 129, 165–176.

Brown, P., Sutikna, T., Morwood, M.J., Soejono, R.P., Jatmiko, Saptomo, E.W., Rokus Awe Due, 2004. A new small-bodied hominin from the Late Pleistocene of Flores, Indonesia. Nature 431, 1055–1061.

Coleman, M.N., Colbert, M.W., 2007. Technical note: CT thresholding protocols for taking measurements on three-dimensional models. Am. J. Phys. Anthropol. 133, 723–725.

Culotta, E., 2005. Discoverers charge damage to "hobbit" specimens. Science 307, 1848.

Day, M.H., Wood, B.A., 1968. Functional affinities of the Olduvai Hominid 8 talus. Man 3, 440–445.

Falk, D., Hildebolt, C., Smith, K., Jungers, W.L., Larson, S.G., Morwood, M.J., Sutikna, T., Saptomo, T., Jatmiko, Prior, F., 2008. LB1 did not have Laron Syndrome. Am. J. Phys. Anthropol. suppl. 46, 95.

Flower, W.H., 1889. Description of two skeletons of Akkas, a pygmy race from Central Africa. J. Anthropol. Inst. Great Britain and Ireland 18, 3–19.

Gebo, D.L., Schwartz, G.T., 2006. Foot bones from Omo: implications for hominid evolution. Am. J. Phys. Anthropol. 129, 499–511.

Grine, F.E., Jungers, W.L., Tobias, P.V., Pearson, O.M., 1995. Fossil *Homo* femur from Berg Aukas, Namibia. Am. J. Phys. Anthropol. 97, 151–185.

Hager, L.D., 1996. Sex differences in the sciatic notch of great apes and modern humans. Am. J. Phys. Anthropol. 99, 287–300.

Harcourt-Smith, W.E.H., Aiello, L.C., 2004. Fossils, feet and the evolution of human bipedal locomotion. J. Anat. (Lond.) 204, 403–416.

Harmon, E.H., 2008. Early hominin greater trochanter shape. Am. J. Phys. Anthropol. suppl. 46, 112–113.

Hershkovitz, I., Kornreich, L., Laron, Z., 2007. Comparative skeletal features between *Homo floresiensis* and patients with primary growth hormone insensitivity (Laron syndrome). Am. J. Phys. Anthropol. 134, 198–208.

Hrdlicka, A., 1898. Study of the normal tibia. Am. Anthropol. 11 (old series), 307–312.

Hrdlicka, A., 1934. Contributions to the study of the femur: the crista aspera and the pilaster. Am. J. Phys. Anthropol. 19, 17–37.

Igbigbi, P.S., Sharrif, M., 2005. The bicondylar angle of adult Malawians. Am. J. Orthoped. 34, 291–294.

Jacob, T., 1967. Some Problems Pertaining to the Racial History of the Indonesian Region. Neerlandia, Utrecht.

Jacob, T., Indriati, E., Soejono, R.P., Hsu, K., Frayer, D.W., Eckhardt, R.B., Kuperavage, A.J., Thorne, A., 2006. Pygmoid Australomelanesian *Homo sapiens* skeletal remains from Liang Bua, Flores: Population affinities and pathological abnormalities. Proc. Nat. Acad. Sci. U.S.A. 103, 13421–13426.

Johanson, D.C., Lovejoy, C.O., Kimbel, W.H., White, T.D., Ward, S.C., Bush, M.E., Latimer, B.M., Coppens, Y., 1982. Morphology of the Pliocene partial hominid skeleton (A.L. 288-1) from the Hadar Formation, Ethiopia. Am. J. Phys. Anthropol. 57, 403–451.

Jungers, W.L., 1982. Lucy's limbs; skeletal allometry and locomotion in *Australopithecus afarensis*. Nature 297, 676–678.

Jungers, W.L., 2009. Interlimb proportions in humans and fossil hominins: variability and scaling. In: Grine, F.E., Fleagle, J.G., Leakey, R.E. (Eds.), The First Humans: Origins of the Genus Homo. Springer, Netherlands, pp. 93–98.

Kidd, R., 1998. The past is the key to the present: thoughts on the origins of human foot structure, function and dysfunction as seen from the fossil record. Foot 8, 75–84.

Landis, E.K., Karnick, P., 2006. A three-dimensional analysis of the geometry and curvature of the proximal tibial articular surface of hominoids. Proc. SPIE 6056, 12 (published on-line).

Langdon, J.H., 1986. Functional morphology of the Miocene hominoid foot. Contrib. Primatol. 22, 1–225.

Larson, S.G., Jungers, W.L., Tocheri, M.W., Orr, C.M., Morwood, M.J., Sutikna, T., Rokhus Due Awe, Djubiantono, T., 2009. Descriptions of the upper limb skeleton of *Homo floresiensis*. J. Hum. Evol. 57 (5), 555–570.

Latimer, B.M., Lovejoy, C.O., Johanson, D.C., Coppens, Y., 1982. Hominid tarsal, metatarsal, and phalangeal bones recovered from the Hadar Formation: 1974-1977 collections. Am. J. Phys. Anthropol. 57, 701–719.

Lordkipanidze, D., Jashashvili, T., Vekua, A., Ponce de León, M.S., Zollikofer, C.P.E., Rightmire, G.P., Pontzer, H., Ferring, R., Oms, O., Tappen, M., Bukhsianidze, M., Agusti, J., Kahlke, R., Kiladze, G., Martinez-Navarro, B., Mouskhelishvile, A., Mioradze, M., Rook, L., 2007. Postcranial evidence from early *Homo* from Dmanisi, Georgia. Nature 449, 305–310.

Lovejoy, C.O., 2005. The natural history of human gait and posture. Part 1. Spine and pelvis. Gait Posture 21, 95–112.

Lovejoy, C.O., Heiple, K.G., 1970. A reconstruction of the femur of *Australopithecus africanus*. Am. J. Phys. Anthropol. 32, 33–40.

Martin, R., Saller, K., 1959. Lehrbuch der Anthropologie, Band II. Gustave Fischer Verlag, Stuttgart.

McFadden, D., Bracht, M.S., 2005. Sex differences in the relative lengths of metacarpals and metatarsals in gorillas and chimpanzees. Hormone and Behavior 47, 99–111.

McHenry, H.M., 1975. A new pelvic fragment from Swartkrans and the relationship between the robust and gracile australopithecines. Am. J. Phys. Anthropol. 43, 245–262.

McHenry, H.M., Jones, A.L., 2006. Hallucial convergence in early hominids. J. Hum. Evol. 50, 534–539.

Morwood, M.J., Brown, P., Jatmiko, Sutikna, T., Saptomo, E.W., Westaway, K.E., Rokus Awe Due, Roberts, R.G., Maeda, T., Wasisto, S., Djubiantono, T., 2005. Further evidence for small-bodied hominins from the Late Pleistocene of Flores, Indonesia. Nature 437, 1012–1017.

Organ, J.M., Ward, C.V., 2006. Contours of the hominoid lateral tibial condyle with implications for *Australopithecus*. J. Hum. Evol. 51, 113–127.

Papadopoulos, C.C., Damon, A., 2005. Some genetic traits in Solomon Island populations. III. Relative toe length. Am. J. Phys. Anthropol. 39, 185–189.

van der Plas, M., 2007. A new model for the evolution of *Homo sapiens* from the Wallacean island. PalArch's J. Vert. Palaeontol. 1, 1–121.

Rauch, A., Thiel, C.T., Schindler, D., Wick, U., Crow, Y.J., Ekici, A.B., van Essen, A.J., Goecke, T.O., Al-Gazali, L., Chrzanowska, K.H., Zweier, C., Brunner, H.G., Becker, K., Curry, C.J., Dallapiccola, B., Devriendt, K., Dörfler, A., Kinning, E., Megarbane, A., Meinecke, P., Semple, R.K., Spranger, S., Toutain, A., Trembath, R.C., Voß, E., Wilson, L., Hennekam, R., de Zegher, F., Dörr, H.-G., Reis, A., 2008. Mutations in the pericentrin (PCNT) gene cause primordial dwarfism. Science 319, 816–819.

Rhoads, J.G., Trinkaus, E., 1977. Morphometrics of the Neandertal talus. Am. J. Phys. Anthropol. 46, 29–44.

Roberts, R.G., Westaway, K.E., Zhao, J.-x., Turney, C.S.M., Bird, M.I., Rink, W.J., Fifield, L.K., 2009. Geochronology of cave deposits at Liang Bua and of adjacent river terraces in the Wae Racang valley, western Flores, Indonesia: a synthesis of age estimates for the type locality of *Homo floresiensis*. J. Hum. Evol. 57 (5), 484–502.

Sarmiento, E.E., Marcus, L.F., 2000. The os navicular of humans, great apes, OH 8, Hadar, and *Oreopithecus*: function, phylogeny and multivariate analysis. Am. Mus. Novitates 3288, 1–38.

Schmitt, A., Wapler, U., Couallier, V., Cunha, E., 2007. Are bone losers distinguishable from bone formers in skeletal series? Implications for adult age at death assessment methods. HOMO 58, 53–66.

Shefelbine, S.J., Tardieu, C., Carter, D.R., 2002. Development of the femoral diaphyseal angle in hominid bipedalism. Bone 30, 765–770.

Singh, S., Potturi, B.R., 1978. Greater sciatic notch in sex determination. J. Anat. (Lond.) 125, 619–624.

Spoor, C.F., Zonneveld, F.W., Macho, G.A., 1993. Linear measurements of cortical bone and dental enamel by computed tomography: applications and problems. Am. J. Phys. Anthropol. 91, 469–484.

Stern Jr., J.T., Susman, R.L., 1983. The locomotor anatomy of *Australopithecus afarensis*. Am. J. Phys. Anthropol. 60, 279–317.

Susman, R.L., 1983. Evolution of the human foot: evidence from Plio-Pleistocene hominids. Foot Ankle 3, 365–376.

Susman, R.L., Brain, T.M., 1988. New first metatarsal (SKX 5017) from Swartkrans and the gait of *Paranthropus robustus*. Am. J. Phys. Anthropol. 77, 7–15.

Susman, R.L., Stern, J.T., Jungers, W.L., 1984. Arboreality and bipedality in the Hadar hominids. Folia Primatol. 43, 113–156.

Tague, R.G., Lovejoy, C.O., 1986. The obstetric pelvis of AL-288-1 (Lucy). J. Hum. Evol. 15, 237–255.

Takahashi, H., 2006. Curvature of the greater sciatic notch in sexing the human pelvis. Anthropol. Sci. 114, 187–191.

Tardieu, C., Damsin, J.P., 1997. Evolution of the angle of obliquity of the femoral diaphysis during growth – correlations. Surg. Radiol. Anat. 19, 91–97.
Trinkaus, E., 1983. The Shanidar Neandertals. Academic Press, New York.
Trinkaus, E., 2006. Modern human versus Neandertal evolutionary distinctiveness. Curr. Anthropol. 47, 597–620.
Trinkaus, E., Ruff, C.B., 1999. Diaphyseal cross-sectional geometry of Near Eastern Middle Paleolithic humans: the tibia. J. Arch. Sci. 26, 1289–1300.
Van Heteren, A.H., 2008. *Homo floresiensis* as an island form. PalArch's J. Vert. Palaeontol. 5, 1–12.
Verhoeven, T., 1958. Proto-Negrito in den Grotten auf flores. Anthropos 53, 229–232.
Walker, P.L., 2005. Greater sciatic notch morphology: sex, age, and population difference. Am. J. Phys. Anthropol. 127, 385–391.
Wallace, I., Demes, B., Jungers, W.L., Alvero, M., Su, A., 2008. The bipedalism of the Dmanisi hominins: pigeon-toed early *Homo*? Am. J. Phys. Anthropol. 136, 375–378.
Wescott, D.J., 2006. Ontogeny of femur subtrochanteric shape in Native Americans and American Blacks and Whites. J. Forensic Sci. 51, 1240–1245.
Wescott, D.J., Cunningham, D.L., 2006. Temporal changes in Arikira humeral and femoral cross-sectional geometry associated with horticultural intensification. J. Arch. Sci. 33, 1022–1036.
White, T.D., 1991. Human Osteology. Academic Press, Inc., San Diego.
White, T.D., WoldeGabriel, G., Asfaw, B., Ambrose, S., Beyene, Y., Bernor, R.L., Boisserie, J.-R., Currie, B., Gilbert, H., Haile-Selassie, Y., Hart, W.K., Hlusko, L.J., Howell, F.C., Kono, R.T., Lehmann, T., Luchart, A., Lovejoy, C.O., Renne, P.R., Saegusa, H., Vrba, E.S., Wesselman, H., Suwa, G., 2006. Asa Issie, Aramis and the origin of *Australopithecus*. Nature 440, 883–889.
Wunderlich, R.E. 1999. Pedal form and plantar pressure distribution in anthropoid primates. Doctoral Dissertation: Stony Brook University.